

# Evolution of the Microstructure and Phase Composition of Materials Based on the Fluorohydroxyapatite–Zirconia–Alumina System during Sintering

V. V. Smirnov\*, A. I. Krylov, S. V. Smirnov, M. A. Goldberg, O. S. Antonova, T. O. Obolkina, A. A. Kononov, and S. M. Barinov

*Baikov Institute of Metallurgy and Materials Science, Russian Academy of Sciences, Leninskii pr. 49, Moscow, 119991 Russia*

\*e-mail: smirnov2007@mail.ru

Received December 6, 2016

**Abstract**—We have studied the influence of the sintering temperature,  $\text{Al}_2\text{O}_3$  additions, and liquid-forming sintering aids on the phase composition and microstructure of fluorohydroxyapatite-based composite ceramic materials containing 20 and 60% zirconia. The addition of alumina has been shown to prevent secondary recrystallization processes during sintering and contribute to stabilization of tetragonal zirconia. The addition of the sintering aid has made it possible to lower the sintering temperature to 1200°C.

**Keywords:** bioceramics, zirconia, fluorohydroxyapatite, alumina, sintering

**DOI:** 10.1134/S0020168517090151

## INTRODUCTION

Promising ceramic materials for the fabrication of bone implants include composites based on hydroxyapatite (HA) (the basic mineral component of bone tissue) or on fluorohydroxyapatite (FHA), a more thermodynamically stable analog, and zirconia, a material that possesses high strength, fracture toughness, and chemical stability [1]. However, the preparation of HA– $\text{ZrO}_2$  and FHA– $\text{ZrO}_2$  composites is a complex technological issue because of the chemical interaction between their components at low temperatures (near 1100–1200°C), below the sintering temperature of the components of the composite materials. Kim et al. [2] were able to sinter materials containing 20 vol %  $\text{ZrO}_2$  to a dense state at 1300°C owing to the addition of 5–10 wt % calcium fluoride. Even though a dense state was achieved, the material had relatively poor mechanical properties (bending strength of 130 MPa and fracture toughness under 1.5 MPa  $\text{m}^{1/2}$ ), which was accounted for by the formation of low-strength, cubic  $\text{ZrO}_2$  as a result of complete zirconia stabilization by the calcium ions present in the additive. In addition, a small amount of calcium zirconate was observed to form as a result of reaction between the components, which was accompanied by HA decomposition. Reaction between the components can be prevented using hot pressing with an additional component: up to 30 wt % alumina [3]. However, the strength of the composite increased only slightly, because of the formation of microcracks

around  $\text{Al}_2\text{O}_3$  particles as a result of the large thermal expansion mismatch between  $\text{Al}_2\text{O}_3$  and HA.

Sintering with no significant reaction between components can be ensured by using sintering aids forming low-temperature melts. This would make it possible to lower the sintering temperature and prevent decomposition processes and the formation of secondary phases in the system under consideration.

The objectives of this work were to lower the sintering temperature by using nanopowders and adding liquid-forming components and examine the effect of alumina on the phase composition and microstructure of the material. The basic phase chosen was FHA, which possesses higher thermal and chemical stability than does HA [4].

## EXPERIMENTAL

FHA– $\text{ZrO}_2$  composite materials were prepared using  $\text{ZrO}_2$  powder with a specific surface area  $S \approx 50$ – $52 \text{ m}^2/\text{g}$  and FHA powder with  $S \approx 150$ – $160 \text{ m}^2/\text{g}$ , both synthesized through precipitation from aqueous salt solutions [5, 6]. These specific surface areas correspond to particle sizes of 18 nm for  $\text{ZrO}_2$  and 12 nm for FHA. Partial stabilization of tetragonal  $\text{ZrO}_2$  (*t*- $\text{ZrO}_2$ ) was ensured by adding 2 mol %  $\text{Y}_2\text{O}_3$ . According to X-ray diffraction data, the resultant powders consisted of *t*- $\text{ZrO}_2$  and FHA with 10% of OH groups replaced by fluorine. Sinterability was evaluated for the compositions indicated in the Table 1.  $\text{Al}_2\text{O}_3$  (5 wt %) in the

**Table 1.** Compositions of the composite materials

Composition, wt %	Notation		
	without additives	5 wt % Al <sub>2</sub> O <sub>3</sub>	5 wt % Al <sub>2</sub> O <sub>3</sub> + sintering aid
40 FHA, 60 ZrO <sub>2</sub>	Z6F4	Z6F4 + A	Z6F4 + A + S1
80 FHA, 20 ZrO <sub>2</sub>	Z2F8	Z2F8 + A	Z2F8 + A + S2

form of aluminum nitrate (analytical grade Al(NO<sub>3</sub>)<sub>3</sub> · 6H<sub>2</sub>O), a water-soluble salt, was added in the ZrO<sub>2</sub> synthesis step (Table 1). To obtain more homogeneous, denser microcrystalline structures, liquid-forming additives were introduced into the ceramic materials. At the higher ZrO<sub>2</sub> content, we used a sodium silicate (Na<sub>2</sub>SiO<sub>3</sub> · 9H<sub>2</sub>O) based additive (5 wt %), S1, developed for zirconia ceramics [5]. In the case of the FHA-rich materials, we used an additive (2 wt %) based on alkali fluorides (NaF–KF eutectic), S2 (Table 1) [6]. The powders (FHA + ZrO<sub>2</sub> or FHA + ZrO<sub>2</sub>–Al<sub>2</sub>O<sub>3</sub>) were mixed by grinding in a planetary mill using zirconia balls. After mixing the powders, the resultant samples were compacted by semidry biaxial pressing at 100–120 MPa in steel dies. The green compacts were then sintered in air in furnaces with silit rod heaters for 1 h at temperatures of 1250 and 1330°C.

The materials were characterized by X-ray diffraction (XRD) analysis (Shimadzu XRD-6000 diffractometer, CuK<sub>α</sub> radiation) using JCPDS Powder Diffraction File and PCPDFWIN data (72-1937 and 72-0506). The specific surface area of the powders was determined by low-temperature nitrogen BET measurements (Micromeritics TriStar analyzer). The bending strength of the ceramics was determined on an Instron 5581 tensile tester (as an average over five specimens). Microstructures were examined by scanning electron microscopy (SEM) on a Tescan VegaII.

## RESULTS AND DISCUSSION

Microstructural examination of the Z2F8 materials showed that even sintering at a temperature as low as 1200°C led to considerable growth of calcium phosphate (CP) crystallites: to 1–10 μm. The porosity of the material was 30–35% and the pore size reached 6–8 μm (Fig. 1a). The large crystallite size and high porosity were a consequence of CP crystallization. Small ZrO<sub>2</sub> crystallites (less than 1 μm in size) were located on the surface of CP grains. It seems likely that the addition of 20 wt % ZrO<sub>2</sub> hinders CP sintering and does not prevent directional growth of large crystallites. The growth of large CP crystallites and microstructural inhomogeneity are caused by the nonuniform distribution of ZrO<sub>2</sub> particles during mechanical mixing of the components. The material containing 60 wt % ZrO<sub>2</sub> (Z6F4) consisted of FHA crystallites ranging in size from 2 to 5 μm (some of the crystallites

were up to 10–15 μm in size) and small ZrO<sub>2</sub> crystallites (1–3 μm). In contrast to Z2F8, it had small pores, with an average size from 1 to 2 μm, and about 25% porosity (Fig. 1b).

According to X-ray diffraction data, the major crystalline phase in the Z2F8 material was monoclinic zirconia (*m*-ZrO<sub>2</sub>). Also present was a small amount (less than 5 wt %) of *t*-ZrO<sub>2</sub> (Fig. 2). The material contained no apatite phase, but there was well-crystallized β-tricalcium phosphate (β-TCP). Raising the sintering temperature to 1330°C led to an increase in the amount of *m*-ZrO<sub>2</sub> and reduced the intensity of the reflections from β-TCP, which is attributable to reaction between the components, resulting in decomposition of phosphate compounds.

X-ray diffraction characterization of the Z6F4 material showed that there was also a tendency for the amount of *m*-ZrO<sub>2</sub> to increase with respect to *t*-ZrO<sub>2</sub> as the sintering temperature was raised from 1200 to 1330°C. Calcium phosphate crystallized as apatite rather than as β-TCP.

The addition of Al<sub>2</sub>O<sub>3</sub> (sintering at 1200°C, Z2F8 + A composite) led to the formation of a microcrystalline structure. The average crystallite size of the CP phase decreased by approximately a factor of 5–10, to about 0.5–4 μm, whereas the porosity of the material remained at a level of 30–35% (Fig. 3a). The considerable decrease in crystallite size is attributable to the uniform distribution of the added Al<sub>2</sub>O<sub>3</sub> over the sample.

The use of a liquid-forming additive (Z2F8 + A + S2) ensures the formation of a considerably denser microstructure, with an about 5% porosity (Fig. 3b). Pores 1–2 μm in size concentrate on crystallite boundaries. The CP crystallites range in size from 2 to 5 μm. The micrograph in Fig. 3b clearly demonstrates regions with zirconia crystallites in the form of sintered aggregates distributed over the sample and spaced several microns apart. The sintered aggregates range in size from 4 to 6 μm and consist of crystallites about 100–200 nm in size. The two major phases are in intimate contact, which points to reaction between the components or mutual dissolution.

After sintering at a temperature of 1330°C, the microstructure of the Z2F8 + A material (Fig. 3c) was similar to that of the Z2F8 + A + S2 material (containing an additive) sintered at 1200°C (Fig. 3b). One distinction is the presence of more elongated pores on the boundaries of the CP crystallites, which range in size

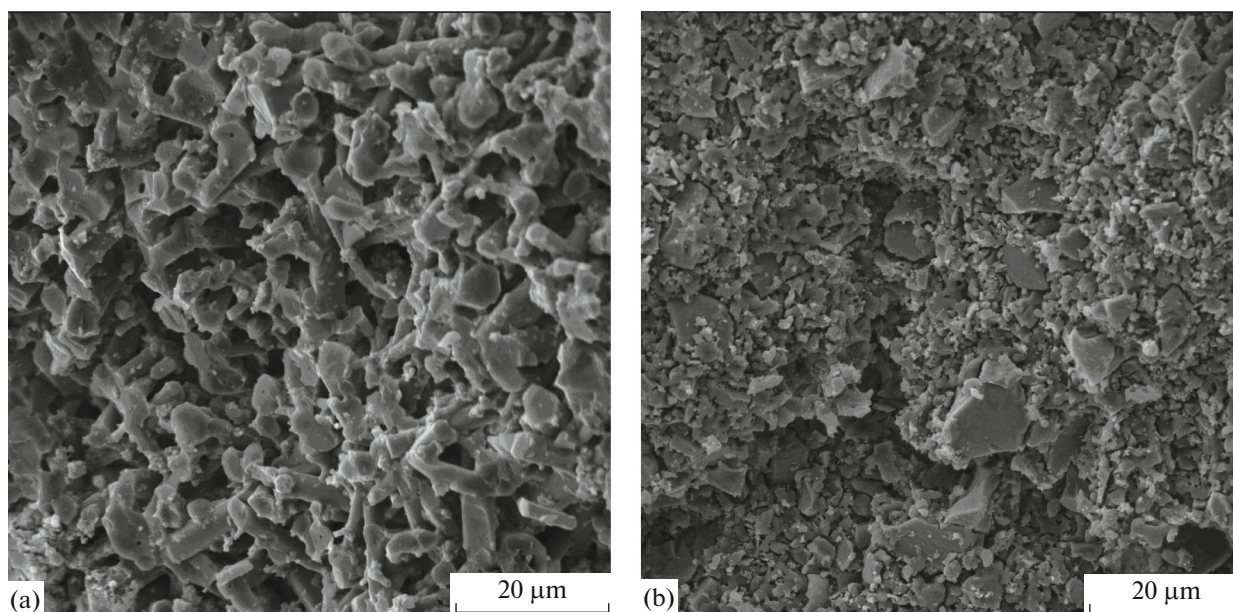


Fig. 1. Microstructures of the (a) Z2F8 and (b) Z6F4 ceramics (sintering at 1200°C).

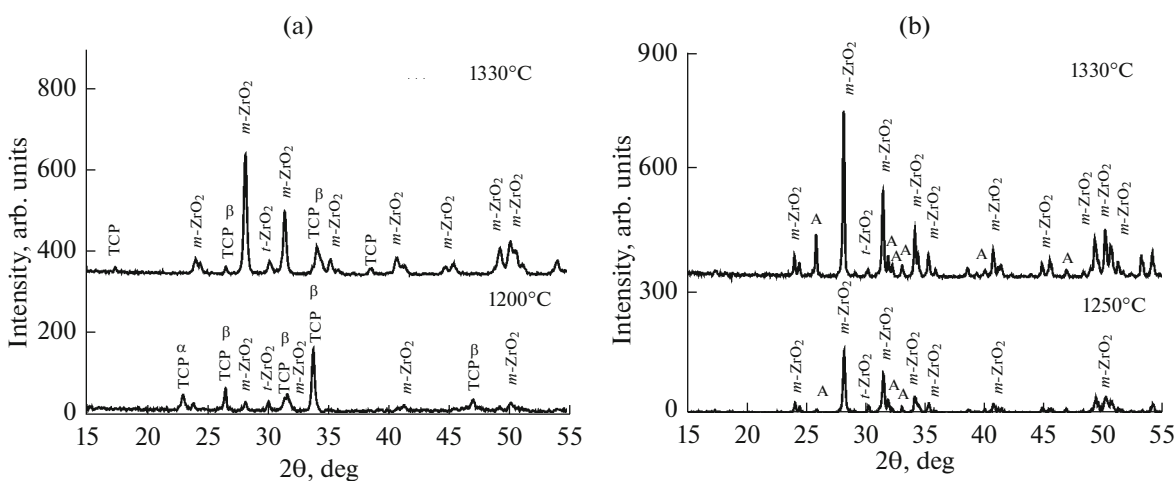


Fig. 2. X-ray diffraction patterns of the (a) Z2F8 and (b) Z6F4 materials sintered at 1200 and 1330°C; A = apatite phase,  $\alpha$  =  $\alpha$ -TCP,  $\beta$  =  $\beta$ -TCP.

up to 4  $\mu\text{m}$ . This demonstrates that the sintering aid ensures more complete sintering even at a temperature of 1200°C.

A similar microstructure was observed in the case of the Z2F8 + A + S2 material sintered at 1330°C (Fig. 3d). This material is distinctive in that it has a coarse microstructure: the crystallites range in size from 3 to 6  $\mu\text{m}$  and are densely packed.

Thus, the most uniform, microcrystalline structure among the apatite-rich materials was obtained at 1200°C with the use of the sintering aid (Z2F8 + A + S2). Raising the sintering temperature to 1330°C led to considerable crystallite growth.

The microstructure of the ZrO<sub>2</sub>-rich, alumina-containing samples (Z6F4 + A) sintered at 1200°C is nonuniform in particle size and has high porosity, up to 30% (Fig. 4a). There are irregularly shaped apatite particles up to 5  $\mu\text{m}$  in size and ZrO<sub>2</sub> crystallites 0.5 to 2  $\mu\text{m}$  in size. The porosity of the samples prepared using a sintering aid (Z6F4 + A + S1, Fig. 4b) is considerably lower, 5–7%, and they have a uniform microstructure with an average CP crystallite size of about 4–5  $\mu\text{m}$  (some of the crystallites are up to 10  $\mu\text{m}$  in size). The ZrO<sub>2</sub> crystallites are about 1–2  $\mu\text{m}$  in size. The materials sintered at 1330°C have higher density. The material prepared with no sintering aid



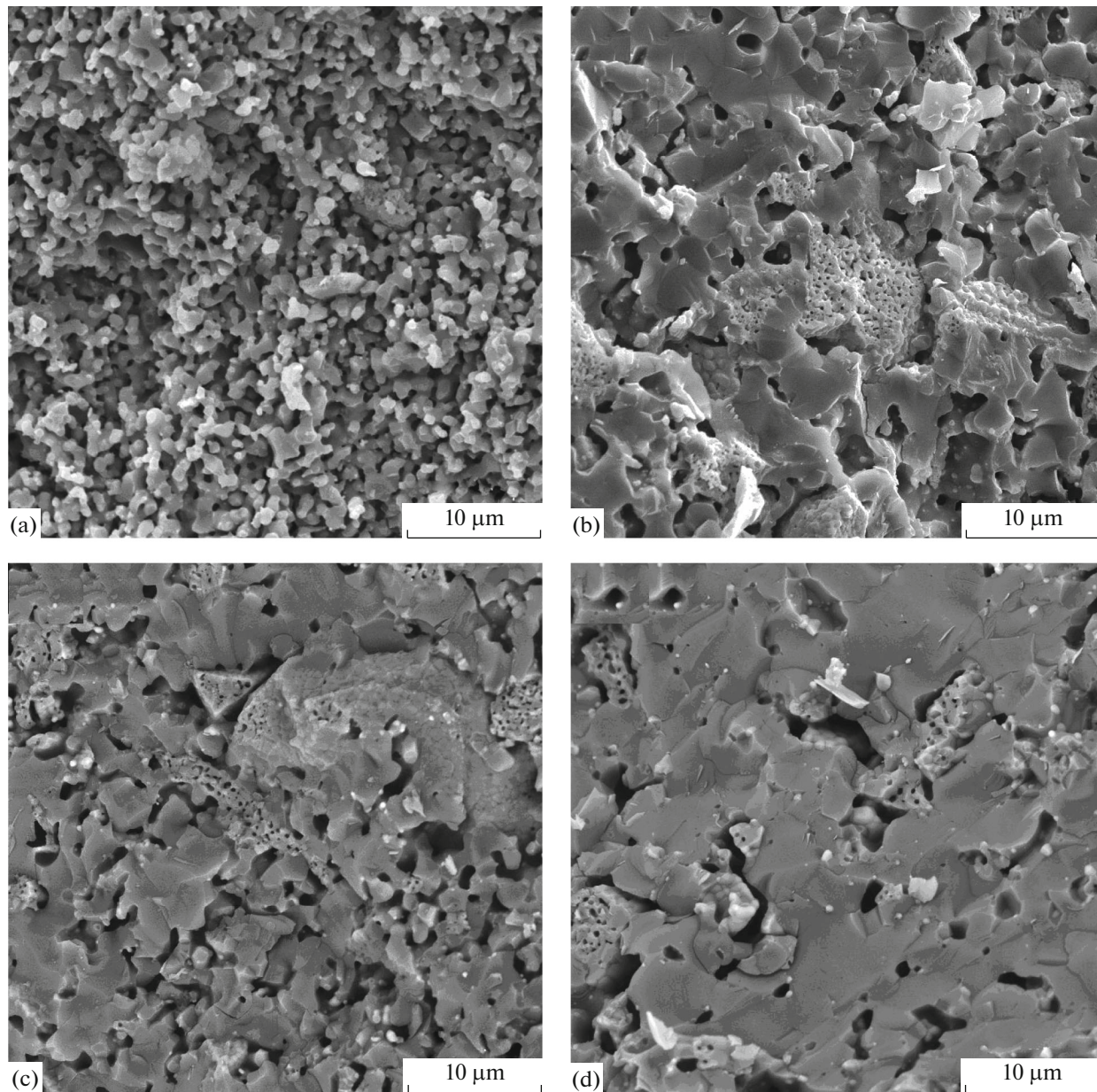


**Fig. 3.** Microstructures of the (a, c) Z2F8 + A (no sintering aid) and (b, d) Z2F8 + A + S2 (sintering aid) ceramics prepared by sintering at (a, b) 1200 and (c, d) 1330°C.

(Z6F4 + A) contains separate pores 1–2  $\mu\text{m}$  in size on crystallites boundaries (Fig. 4c). The crystallites range in size from 2 to 5  $\mu\text{m}$ . The large crystallites consist of calcium phosphate compounds and the small crystallites (0.2–1  $\mu\text{m}$ ) consist of  $\text{ZrO}_2$ . Thus, raising the sintering temperature helped to reduce porosity, whereas the crystallite size of both phases remained almost unchanged. The densest materials were obtained at a temperature of 1330°C in the presence of a sintering aid (Z6F4 + A + S1, Fig. 4d). The material is essentially free of pores and consists of densely packed crystallites. The two phases present differ in crystallite shape: large, irregularly shaped crystallites 1–3  $\mu\text{m}$  in

size (CP) and small crystallites 0.5 to 1  $\mu\text{m}$  in size ( $\text{ZrO}_2$ ).

In the X-ray diffraction patterns of the  $\text{ZrO}_2$ –FHA– $\text{Al}_2\text{O}_3$  composites, no reflections from  $\text{Al}_2\text{O}_3$  or any other aluminum compound were detected. It seems likely that the alumina dissolves in the other components of the system.

The Z2F8 + A material sintered at 1200°C consisted predominantly of *t*- $\text{ZrO}_2$  and an apatite phase. Also present were small amounts of *m*- $\text{ZrO}_2$  and TCP. In the Z6F4 + A material, a major phase was *t*- $\text{ZrO}_2$ .



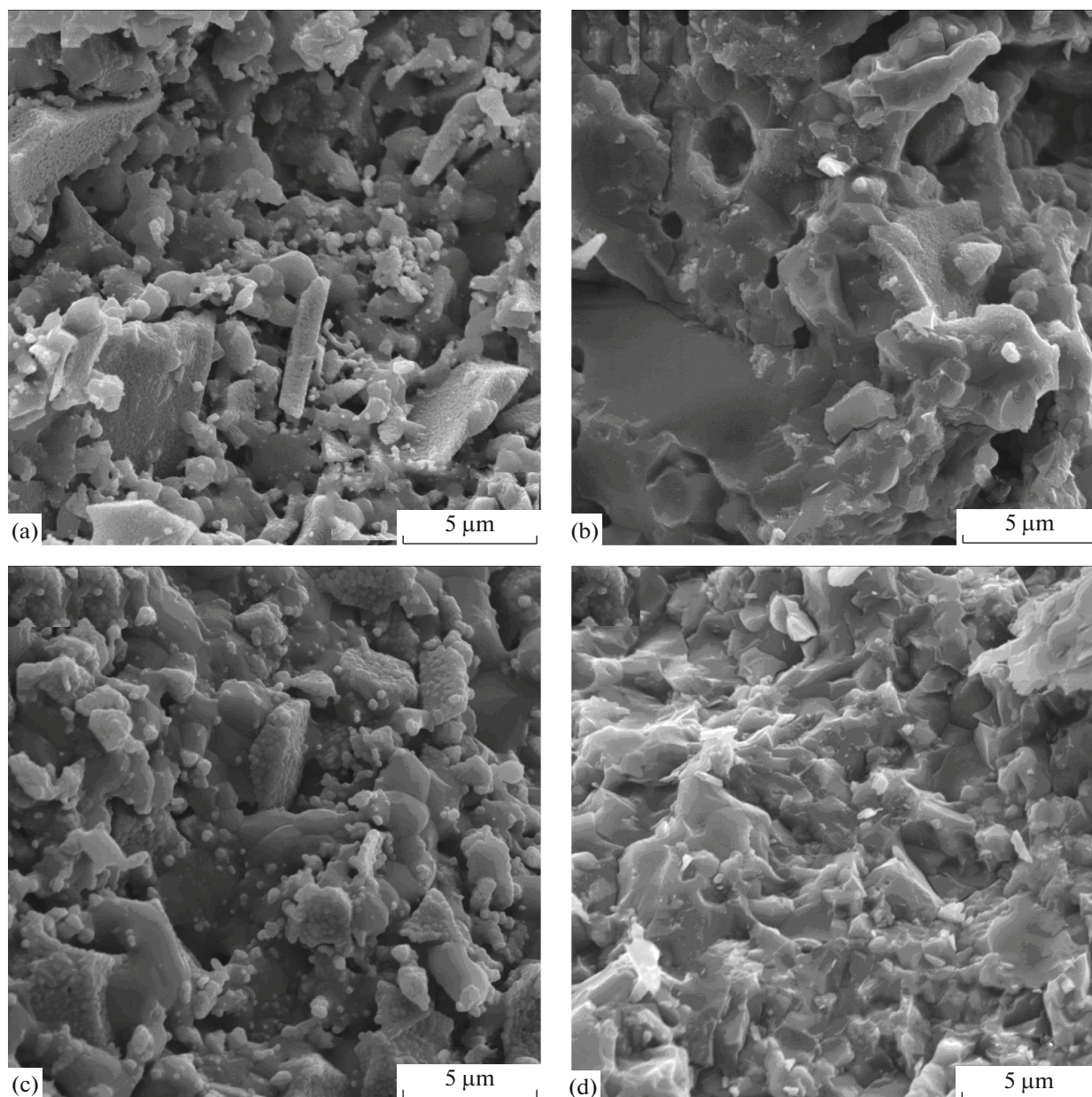


**Fig. 4.** Microstructures of the Z6F4 + A ceramics (a, c) without and (b, d) with a sintering aid; sintering at (a, b) 1200 and (c, d) 1330°C.

The other phases (CP and  $m$ -ZrO<sub>2</sub>) were present in smaller amounts (Fig. 5).

The addition of the sintering aids changed the relative amounts of the zirconia polymorphs. The addition of the S2 sintering aid to the FHA-rich material (Z2F8 + A + S2) led to a considerable decrease in  $m$ -ZrO<sub>2</sub> concentration, to the point of complete disappearance, that is, the sintering aid had a stabilizing effect on cubic ZrO<sub>2</sub> ( $c$ -ZrO<sub>2</sub>). No significant effect of the sintering aid on the apatite phase or TCP was detected. In the Z6F4 + A + S1 composite, the sintering aid favored the formation of  $m$ -ZrO<sub>2</sub> and reduced the per-

centage of  $t$ -ZrO<sub>2</sub>. The apatite phase disappeared, and TCP emerged instead (Fig. 5).

After sintering at 1330°C, the Z2F8 + A material consisted of the following phases:  $t$ -ZrO<sub>2</sub>, apatite phase, and TCP. In the Z6F4 + A material, zirconia was present as a mixture of  $t$ -ZrO<sub>2</sub> and  $c$ -ZrO<sub>2</sub>. The other phases—TCP and apatite—were present in small amounts (Fig. 6).

The addition of the sintering aid (Z2F8 + A + S2) led to a decrease in the percentage of  $t$ -ZrO<sub>2</sub>. This can be accounted for by partial dissolution of zirconia in the liquid additive at the high sintering temperature

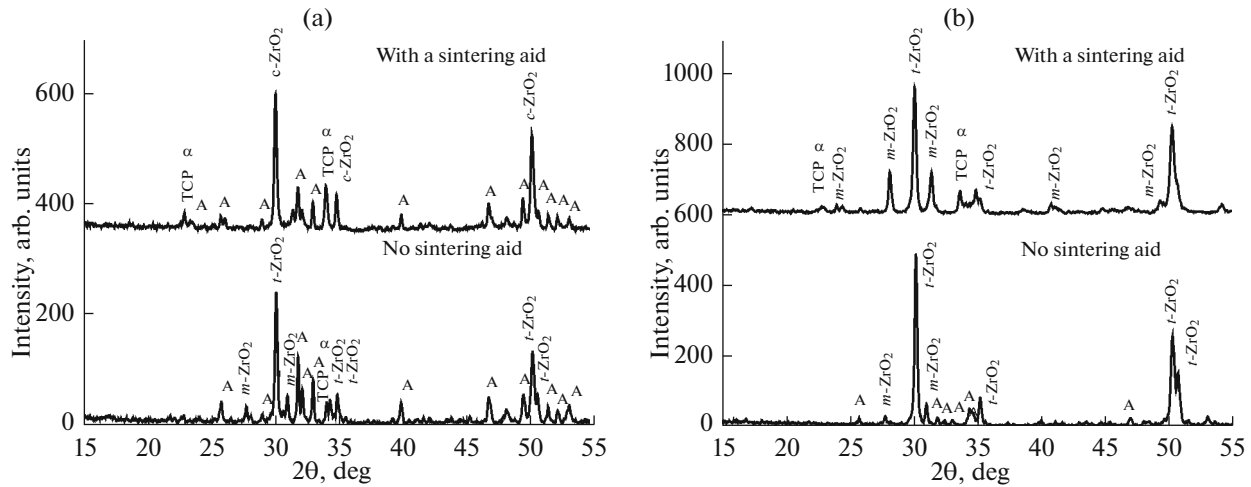


**Fig. 5.** X-ray diffraction patterns of the (a) Z2F8 + A, Z2F8 + A + S2, (b) Z6F4 + A, and Z6F4 + A + S1 materials prepared by sintering at 1200°C; A = apatite phase,  $\alpha = \alpha$ -TCP.

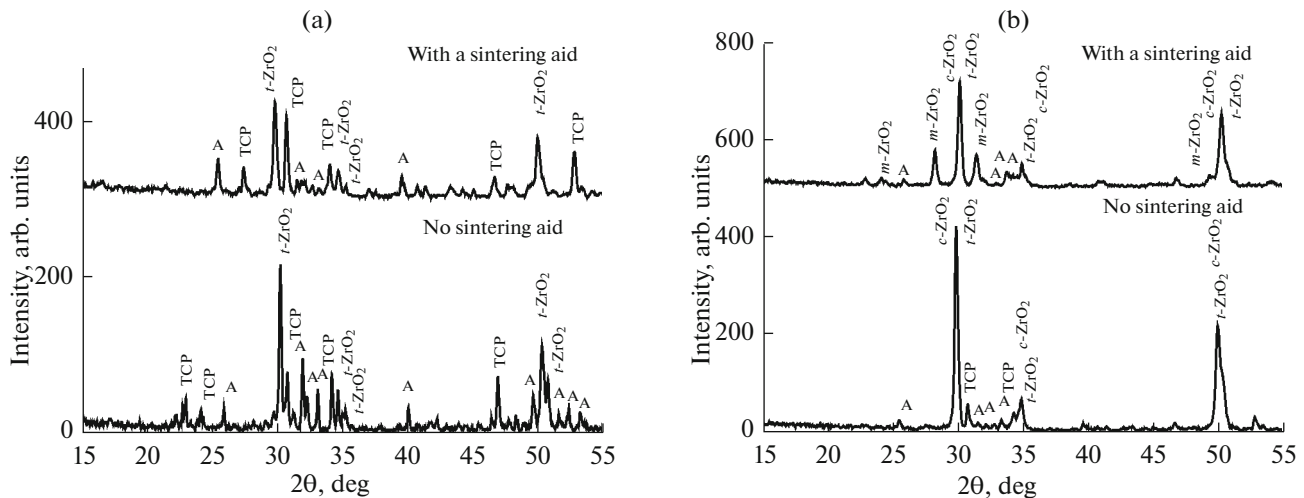


**Fig. 6.** X-ray diffraction patterns of the (a) Z2F8 + A, Z2F8 + A + S2, (b) Z6F4 + A, and Z6F4 + A + S1 materials prepared by sintering at 1330°C; A = apatite phase,  $\alpha = \alpha$ -TCP,  $\beta = \beta$ -TCP.

(1330°C) and subsequent formation of an amorphous phase during cooling. Moreover, the sintering aid led to a reduction in the intensity of the reflections from the apatite phase and an increase in the intensity of the reflections from TCP. This is attributable to partial recrystallization of the apatite phase to TCP. In contrast to Z2F8 + A + S2, the zirconia-rich material Z6F4 + A + S1 contained roughly equal amounts of *t*-ZrO<sub>2</sub> and *m*-ZrO<sub>2</sub>. The amount of the calcium phosphate phases also decreased, and there were no reflections from TCP. This can also be accounted for by the formation of melts based on liquid sodium silicate, with partial CP dissolution in it.

Thus, the sintering aids influence the phase composition of the material because of the dissolution of

its components in the liquid phase, whose amount increases with increasing temperature.

The sintering aids and alumina were found to raise the strength of the materials. In particular, after sintering at a temperature of 1330°C the bending strength of the Z2F8 material was 35–40 MPa and that of the Z2F8 + A material was 65–70 MPa. The strength gain on the addition of Al<sub>2</sub>O<sub>3</sub> is due to the formation of a more uniform, microcrystalline structure. The Z2F8 + A + S2 material had an even higher strength: 125–143 MPa after sintering at 1200°C. This is attributable to the formation of a microstructure with densely packed crystallites and low porosity even at low sintering temperatures.

The zirconia-rich materials (Z6F4 + A + S1) had the highest strength after sintering at a temperature of

1330°C: 370 MPa. This is attributable to the higher content of the high-strength phase *t*-ZrO<sub>2</sub> in comparison with Z2F8 + A + S2 and to the dense, uniform, microcrystalline structure of these materials, with porosity as low as 1%.

### CONCLUSIONS

The present results on the sintering of ceramic materials in the ZrO<sub>2</sub>–FHA–Al<sub>2</sub>O<sub>3</sub> system at 1200 and 1330°C demonstrate that the addition of alumina helps to obtain a more uniform, microcrystalline structure and increase the percentage of tetragonal ZrO<sub>2</sub>. Sintering is accompanied by a partial conversion of the apatite phase to TCP. The addition of liquid-forming sintering aids helps to reduce the porosity of the materials. The densest materials (Z6F4 + A + S1), with porosity below 1%, have been obtained by sintering at 1330°C.

### ACKNOWLEDGMENTS

This work was supported by the Russian Foundation for Basic Research, grant no. 14-08-00575.

### REFERENCES

1. Heuer, A.H., Fracture-tough ceramics: the use of martensitic-toughening in ZrO<sub>2</sub>-containing ceramics, *Mater. Sci. Monographs*, 1985, vol. 26, pp. 264–278.
2. Kim, H.W., Koh, Y.H., Yoon, B.H., and Kim, H.E., Reaction sintering and mechanical properties of hydroxyapatite–zirconia composites with calcium fluoride additions, *J. Am. Ceram. Soc.*, 2002, vol. 85, no. 6, pp. 1634–1636.
3. Kong, Y.M., Kim, S., Kim, H.E., and Lee, I.S., Reinforcement of hydroxyapatite bioceramic by addition of ZrO<sub>2</sub> coated with Al<sub>2</sub>O<sub>3</sub>, *J. Am. Ceram. Soc.*, 1999, vol. 82, no. 11, pp. 2963–2968.
4. Barinov, S.M. and Komlev, V.S., *Biokeramika na osnove fosfatov kal'tsiya (Calcium Phosphate-Based Bioceramics)*, Moscow: Nauka, 2005.
5. Smirnov, V.V., Smirnov, S.V., Krylov, A.I., Antonova, O.S., Goldberg, M.A., Shvorneva, L.I., Titov, D.D., Medvecky, L., Baikin, A.S., and Barinov, S.M., Ceramics based on zirconia with a low sintering temperature, *Powder Metall. Prog.*, 2014, vol. 14, no. 3, pp. 148–156.
6. Smirnov, V.V., Kochanov, G.P., Antonova, O.S., Shvorneva, L.I., and Barinov, S.M., Effect of  $\gamma$ -irradiation on sintering of fluorohydroxyapatite ceramics, *Dokl. Chem.*, 2012, vol. 446, no. 1, pp. 193–195.

*Translated by O. Tsarev*